The paper was published in the proceedings of the 11th International Conference on Physical Modelling in Geotechnics (ICPMG2026) and was edited by Ioannis Anastasopoulos. The conference was held from June 8th to June 12th 2026 in Zurich, Switzerland.

Centrifuge Modelling Approach to Assess Soil Thermal Properties

M. P. J. Dayana
University of Sheffield, UK, mdpj1@sheffield.ac.uk

E. T. Bowman
University of Sheffield, UK, e.bowman@sheffield.ac.uk

T. A. V. Gaspar
Imperial College London, UK, t.gaspar@imperial.ac.uk

ABSTRACT: Climate change has increased the amount of solar radiation reaching the Earth's surface, contributing to rising temperatures and posing potential risks to geotechnical infrastructure. The thermal properties of soil are governed by a complex interplay of soil micro- and macro-scale features, and the energy input it receives. This study presents a laboratory investigation of thermal gradient development in sand using centrifuge testing through radiative heating using infrared and visible light heat lamps replicating diurnal variations under varying gravitation conditions (20g and 40g). The thermal response of cylindrical sand models with different surface albedo treatments was analysed using thermocouples installed at predefined depths, with higher sensor density near the soil surface. Comparative 1g tests were also conducted to isolate the effects of gravitational forces on thermal gradients in soil. Under 1g conditions, the observed thermal response deviated from expectations based solely on albedo. Increasing the gravitational level to 20g and 40g introduced strong forced convection within the centrifuge, leading to a substantial reduction in effective radiative heat input, as confirmed by decreasing pyranometer readings with increasing Ng. Under these conditions, air temperature fluctuations were moderated, and albedo-driven differences in soil temperature became more pronounced, with the dark-coloured column consistently exhibiting higher surface and subsurface temperatures. Experiments under IR irradiation showed trends similar to VL irradiation but at higher temperature magnitudes due to greater infrared absorption. Across all conditions, thermal effects were largely confined to the near-surface region, with the strongest temperature gradients occurring within the upper 0.5 m of soil.

1 INTRODUCTION

According to the Intergovernmental Panel on Climate Change (IPCC) report (IPCC, 2023) report, the global average near-surface temperature over the last decade was approximately 1.1–1.2°C above pre-industrial (1850–1900) levels, with some individual years exceeding 1.2°C. Global surface temperatures are expected to continue rising until at least mid-century under all emission scenarios considered (IPCC, 2023). These rising air temperatures can significantly alter soil behaviour (Brandon and Mitchell, 1989; Laloui, 2001; Coccia and McCartney, 2016; Casarella, Tarantino and Di Donna, 2020; Loria and Coulibaly, 2021). Soil temperature fluctuates diurnally and seasonally, with diurnal variations fading within tens of centimetres and seasonal variations stabilizing at greater depths. Heat transfer in soil occurs through a multitude of processes including conduction, convection, radiation, mass transfer, evaporation and condensation. However, conduction is generally the dominant mechanism for transferring heat from higher to lower energy sites, particularly through grain-to-grain contacts (Murashov and White, 2000). The role of convection in heat transfer mechanism becomes prominent when there is substantial fluid flow. The rate at which heat is exchanged is determined by the thermal properties of the soil: thermal conductivity and thermal diffusivity (Ali *et al.*, 2024). Thermal conductivity is the capacity of a material to conduct or transmit heat, whilst thermal diffusivity describes the rate at which heat is conducted through a medium. These parameters are strongly influenced by the relative quantity and distribution of solid particle, air and water content, each possessing distinct values. Compared to clay minerals, sands rich in quartz exhibit 15 times greater thermal conductivity than that of water. In general, the thermal conductivity increases with water content, until a threshold is reached, after which it remains relatively constant. In sands, this transition occurs abruptly at low degrees of saturation (typically 5–10 %). Similarly, increased soil density enhances thermal conductivity by increasing particle contact and reducing air-filled voids (Brandon and Mitchell, 1989; Smits *et al.*, 2010). However, the rate of heat transfer due to radiation is strongly influenced by the albedo effect, as darker surfaces absorb more heat than lighter ones (Warke and Smith, 1998).

In natural systems, the Sun emits shortwave radiation, which is partially reflected in the atmosphere or at the soil surface and partially absorbed in the soil. The solar radiation absorbed at the soil surface either provides energy for phase changes or contributes to increased soil temperatures and enhanced ground heat flux (Campbell and Norman, 1998). Thus, soil-atmosphere interaction encompasses the transfer of energy, mass, and momentum between the soil and the atmosphere above it (Blight, 2013). In moist soils, net surface radiation is mainly partitioned into latent heat flux and sensible heat flux. As soils dry, reduced evaporation shifts energy from latent to sensible heat. Once a critical dryness threshold is reached, latent heat flux largely ceases and most radiative energy is converted to sensible heat, producing strong positive thermal feedback to atmosphere (Benson and Dirmeyer, 2021). Understanding how soil moisture influences the thermal gradient is increasingly important in the context of global warming, as changes in temperature and precipitation can modify heat distribution in soils, affecting land–atmosphere interactions and climate feedback. While numerous studies have examined soil thermal behaviour under varying conditions, relatively few have investigated how differences between 1g laboratory experiments and Ng gravitational conditions affect the development of thermal gradients in soils.

This study provide a comprehensive investigation into the thermal behaviour of sand under radiative heating conditions in high gravity conditions. Centrifuge modelling allows investigation of soil thermal behaviour under prototype stress conditions and the associated forced convection, which cannot be reproduced in conventional 1g laboratory tests. This work integrates radiation as a primary heating mechanism and examine its influence through centrifuge testing. By systematically evaluating the effects of different heat lamps, surface albedo treatments, and elevated gravitational fields, the study offers new insights into the coupled thermal processes governing sand behaviour. The comparative approach adopted enables a clearer understanding of how surface and subsurface factors interact to control thermal gradients, thereby advancing current knowledge of soil–atmosphere energy exchange.

2 EXPERIMENTAL SET-UP

The experimental set-up primarily comprised two cylindrical columns, lamp holders, and connecting platforms. Each column had an internal diameter of 100 mm and a height of 200 mm and was fabricated from 5 mm thick PVC pipe. The lamp holder consisted of a custom-designed fixture with angled sides. The front and back of the fixture were enclosed with perforated aluminium sheets to promote airflow and prevent overheating. The fixture was mounted on a metallic plate incorporating a circular opening slightly smaller than the column diameter. This opening served a dual purpose: enabling direct radiation from the lamp onto the top surface of the sand column while preventing direct heating of the PVC pipe under elevated temperature conditions. The two columns were connected using a pair of vertically aligned acrylic plates with circular openings matching the outer diameter of the columns, allowing the columns to be securely slotted in place and preventing lateral movement during testing. This configuration ensured that heat was applied only to the exposed top surface of the sample, minimising lateral heat transfer and promoting one-dimensional vertical heat propagation. A sufficient gap was maintained between the plates to permit airflow during testing, thereby reducing excessive heat build-up and preventing damage to the experimental set-up.

3 CENTRIFUGE SCALING LAWS

The centrifuge facility at the University of Sheffield is a 50g-ton beam drum centrifuge with a radius of 2 m, capable of generating a maximum acceleration of up to 150 g at a payload of 330 kg and 100g at 500 kg. Centrifuge modelling of geotechnical problems enables the reproduction of prototype stress conditions within small-scale models. To translate measurements obtained from centrifuge tests to their equivalent prototype values, a set of scaling laws must be applied. Table 1 summarises the key scaling relationships relavent to this work (Askarinejad *et al.*, 2012; Madabhushi, 2017).

Table 1. Centrifuge scaling laws

Parameter	**Model/Prototype**
Length	1/N
Density	1
Time (Diffusion)	$1/N^2$
Heat flow	N

The results for the Ng cases in Section 6.3.2 are presented in terms of prototype scale.

4 MATERIALS

HST95 light brown silica sand was used in this study. It is a glacial deposit from the Pleistocene Period, sourced from Congleton, Cheshire, England. The sand has an average grain size of 148 µm and predominantly sub-rounded particles. The maximum and minimum dry densities were determined to be 1710 kg/m³ and 1350 kg/m³, respectively. For heat source, 120 W visible light (VL) lamp and 150 W infrared (IR) lamp were used. Temperature was measured using eight thermocouples (TC) per sand column: seven embedded within the column, and one positioned above to measure the air temperature. The buried TCs were installed at depths of 5, 10, 20, 30, 50, 100, and 195 mm from the top surface. All TCs were connected to a National Instruments CompactDAQ (NI cDAQ) chassis, which served as the data acquisition (DAQ) system. In addition, a pyranometer was installed beneath one of the lamp fixtures and near to the soil surface to measure the incident irradiance from the heat source, expressed as power per unit area (W/m²).

5 METHODOLOGY

Two cylindrical sand columns (A and B) were prepared at the same target dry density achieving a dense state. Prior to sand filling, TCs were secured to the inner wall of each column using adhesive and bent into an L-shape so that the sensing junction was positioned at the column centre. Sand was then placed in layers and compacted by tamping, carefully embedding the thermocouples at their designated depths without disturbing their positions. To investigate surface albedo effects, the top 0.5 mm of Column A and B was filled with sand dyed white and black, respectively, using Dr. Ph. Martin's Bombay ink. For the purposes of this study, the white and black-topped columns are labelled as light (L) and dark (D) columns. The degree of brightness was measured using ImageJ software. VL heat lamp was mounted above the columns as the heat source. A pyranometer was positioned on the metal plate and adjacent to the side of the black-dyed colum, almost matching with the sand column top. The test setup was placed inside a strong box for spinning, without a top plate which allow airflow within the chamber. Centrifuge testing was conducted at 20g and 40g to simulate diurnal heating cycles (12 h light/12 h dark) over 28 days, with ON/OFF lamp intervals of 108 s and 27 s corresponding to 20g and 40g, respectively. The lamps were switched ON simultaneously with the initiation of spinning. It is also to be noted that the spinning transitioned directly to 40g without stopping after 20g. Following completion of the VL lamp tests, the heat sources were replaced with IR lamps, and the centrifuge testing procedure was repeated. Before each test, the sand samples were allowed to cool to ambient temperature, ensuring that no residual thermal effects from previous irradiation remained. Test were also conducted without spinning the centrifuge (i.e., under 1g condition) for 60 min with VL lamps ON/OFF at intervals of 108 s. This allows for a comparison between the 1 g and 20 g VL results. However, the comparison may not be direct, as the strong box was not covered with a top plate; consequently, wind effects during spinning likely played a significant role in the Ng results. Photographs of different experimental procedure along with test set-up is shown in Figure 1.

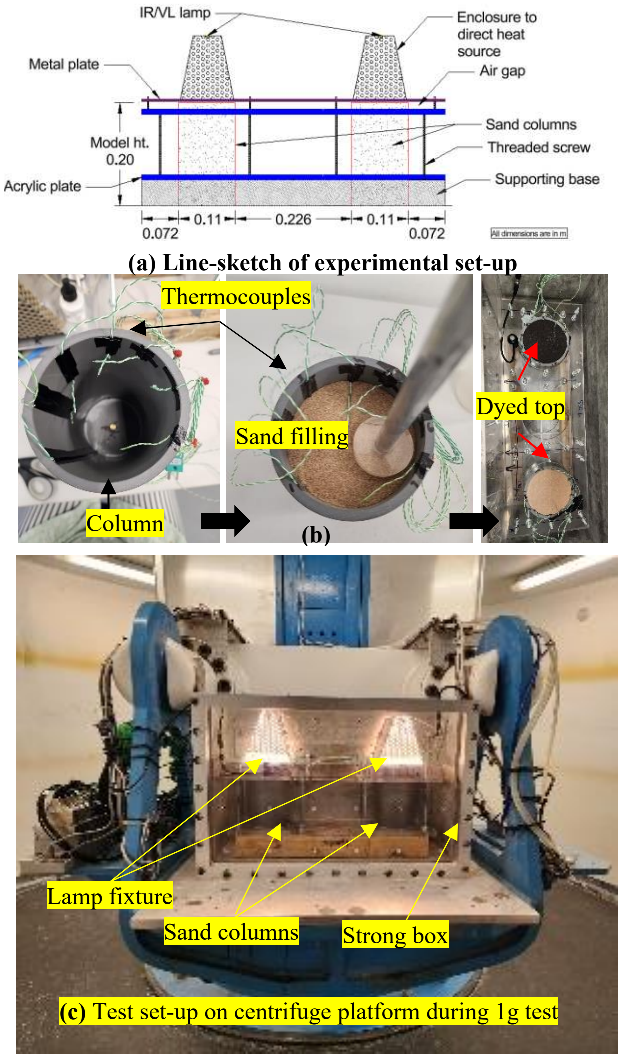

Figure 1. (a) Line sketch of test set-up; (b-c) Photographs of experimental procedures and test set-up.

6 TEST RESULTS

6.1 Model Properties

Both sand columns were prepared using dry sand, resulting in relative densities of 75% and 78%, respectively. Although a minor density variation exists between the two column, both fall within the dense sand range (Mitchell and Soga, 2005) and are therefore expected to exhibit comparable density-dependent behaviour during testing.

To investigate albedo effects, the uppermost 0.5 mm layer of sand was dyed black and white prior to compaction. The black ink was readily absorbed by the sand and retained its colour after washing, whereas the white ink was only partially absorbed, even after prolonged exposure. Nevertheless, the white-dyed sand was used following washing and air-drying.

The surface darkness of the treated sands was quantified using image analysis in ImageJ. Photographs of the black- and white-dyed sands were captured under identical lighting conditions to avoid variations in perceived brightness. Grayscale intensity histograms (ranging from 0 for pure black to 255 for pure white) were obtained using the ImageJ histogram function as shown in Figure 2. The black-dyed sand exhibited a mean grayscale value of 84, compared to 193 for the white-dyed sand, confirming a substantially darker surface. Quantitatively, the black-dyed sand was approximately 2.3 times darker than the white-dyed sand, thereby establishing a clear contrast in surface albedo for the experiments.

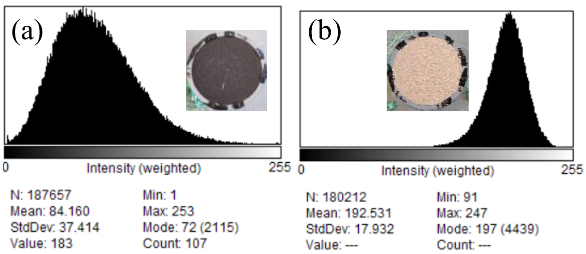

Figure 2. Grayscale intensity histograms of: (a) black-dyed-sand top; (b) white-dyed sand top

6.2 Radiation Energy

The pyranometer readings fluctuated as the lamps were switched ON and OFF. However, the results were not consistent, as shown in Figure 3. Under 1g conditions, when the VL lamp was ON, the measured radiation increased from 820 to 860 W/m² within 60 min. In contrast, at 20g with the VL lamp, the radiation decreased from 795 to 618 W/m², and further spinning to 40 g resulted in a drop to 563 W/m². Under IR radiation, at 20g, the measured radiation showed a slight increase from 640 to 675 W/m² but decreased to 628 W/m² at 40g. In all cases, a significant reduction in heat energy was observed compared to the 1g VL lamp condition. Although the positions of the pyranometer and lamps were fixed, the wind effect generated by centrifuge spinning reduced the heat energy received, and this effect became more pronounced with increasing Ng. Under 20 g and 40 g spinning, the column would have been subjected to approximate wind speeds of 18 m/s and 26 m/s, respectively. This could influence the soil temperature measurements, making direct comparisons between 1 g and Ng results potentially misleading.

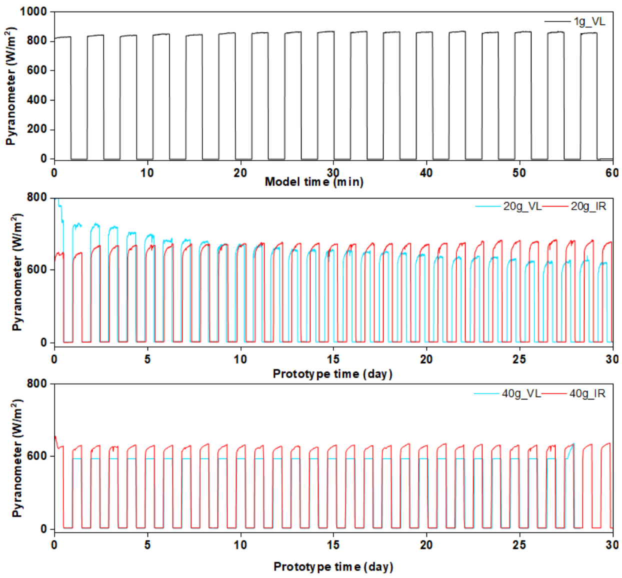

Figure 3. Pyranometer reading during test

6.3 Thermal Effects

TCs measured temperatures both above and below the soil column. Rapid temperature fluctuations were observed in the air and in the shallow (0.5 mm) TCs, so these data are presented separately. For TCs placed at greater depths, temperature changes over time are shown as a function of depth for 0, 2, 5, 10, 15, 20, and 28 days on a prototype scale. The results are shown in Figure 4 and 5 along with a temperature contour plot. Each test was performed on individual days giving ample time for equilibriation with ambient temperature about 18 °C.

6.3.1 Thermal Behaviour: 1g, Visible Light

Under 1g conditions, the thermal response differed from expectations based solely on albedo effects. While a higher temperature gradient was anticipated in the dark-coloured column due to greater radiative absorption, in turn it resulted in a comparable temperature profile in both columns, with the light-coloured surface exhibiting marginally higher temperatures, likely due to weak and inconsistent near-surface convection under 1g conditions.

Air temperature responded directly to the ON–OFF cycling of the irradiation source. The air above the light-coloured column exhibited larger cyclic variations between 20 to 63°C, whereas fluctuations above the dark-coloured surface were limited to between 20 to 50°C.

Consistent behaviour was observed in the near-surface soil temperature measured at a depth of 5 mm. Temperature fluctuations closely followed the lamp cycling and were more pronounced for the light-coloured surface, suggesting a stronger surface–air thermal interaction compared to the dark surface. Despite these differences in transient response, unlike the air temperature, the surface temperature in both cases increased monotonically with time at a faster rate, rising from 18 °C to approximately 85 °C by the end of the experiment.

A rapid rise in surface temperature was observed during the initial heating phase, with temperatures increasing from 18 °C to 50 °C within the first 10 min and then diminished beyond 20 min. Within the soil column, temperature variations were predominantly confined to the upper 50 mm, beyond which they decreased sharply and remained essentially unchanged. This indicates that the imposed thermal boundary conditions primarily affected the near-surface region, with minimal heat propagation into the deeper layers over the duration of the experiment.

6.3.2 Thermal Behaviour: Ng, VL heat lamp

The pattern of temperature variation under 20g conditions was similar to that observed at 1g, but with a markedly lower magnitude. Air temperatures above both columns exhibited a gradual upward trend over time from 20 to 35 °C. In either case, lower than the 1g case, attributed primarily to the forced airflow generated within the centrifuge, as also reflected in the pyranometer readings. Soil surface temperature behaviour differed between columns. The light-coloured column exhibited a large cyclic variation of ~25 °C, with a slower rate of increase, whereas the dark-coloured column showed a rapid rise from 20 to 50 °C during the first 10 days of the prototype period, followed by a slower increase to 55°C within 20 days.

Unlike the 1g results, soil temperatures under 20g conformed to expectations based on albedo, with the dark column producing a higher thermal gradient than the light column. This difference was most pronounced within 0.5 m depth and decreased sharply up to 2 m, where both columns reached comparable temperatures approximately 2 °C above the initial soil temperature. The results indicate that under high-g conditions, enhanced convective mixing in the centrifuge atmosphere moderates surface air temperatures, while subsurface thermal gradients are dominated by intrinsic radiative absorption and soil thermal properties.

Interesting results were obtained under 40g spinning, which generated stronger airflow compared to the 20g condition. A sudden drop in air temperature of ~5 °C was observed above the light-coloured column, while the air above the dark-coloured column exhibited a sharp increase of ~17 °C, yet producing cyclic pattern. A similar pattern was reflected in the light-coloured soil surface temperatures which showed a pronounced dip of ~11 °C, whereas the dark-coloured surface displayed a gradual decreasing trend.

Within the soil, both the light- and dark-coloured columns showed negligible temperature variation over time, remaining consistent with the temperatures recorded during the previous 20g spin. A pronounced temperature difference between the columns was observed within the upper 0.5 m of the prototype, which gradually decreased with depth. Beyond 4 m, both columns exhibited nearly identical temperatures.

6.3.3 Thermal Behaviour: Ng, IR heat lamp

The thermal response under the IR lamp was qualitatively similar to that observed under the visible light (VL) lamp, but with higher temperature magnitudes. Air temperatures above both columns fluctuated between 20 and 40 °C in response to lamp ON–OFF cycling. During continuous 40g spinning, the air temperature above the light column dropped by ~8 °C, whereas the air above the dark column increased sharply by ~20 °C.

Soil surface temperatures under 20g spinning increased from 20 to 50 °C in the light column and from 20 to 70 °C in the dark column. Increasing the spin to 40g induced a sudden reduction of ~6 °C in both columns, followed by a gradual decline over the test period.

Within the soil column, temperature variations were most pronounced within the upper 0.5 m and decreased sharply with depth. Beyond 2 m under 20g and 4 m under 40g, temperatures remained nearly constant. Across all conditions, the dark column consistently exhibited higher temperatures both temporally and with depth, reflecting its greater radiative absorption.

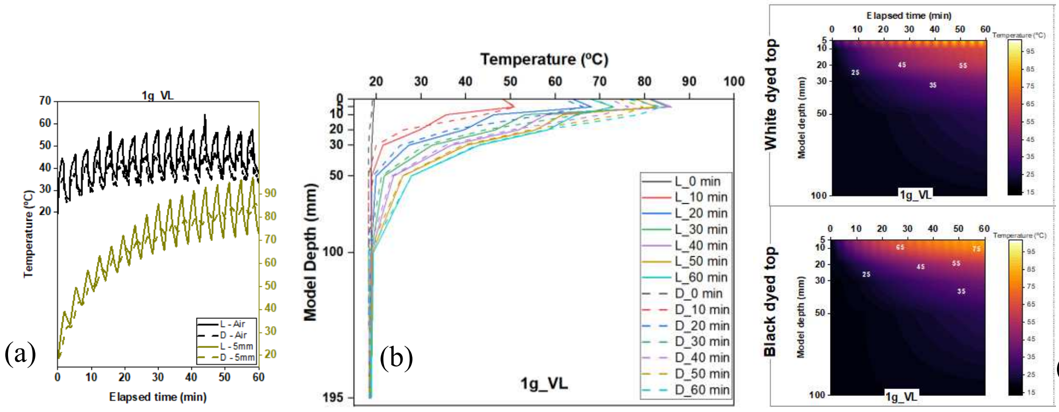

Figure 4. Thermal profiles in 1g with VL heat lamp: (a) temperature vs time; (b) temperature vs depth; (c) heat contour map.

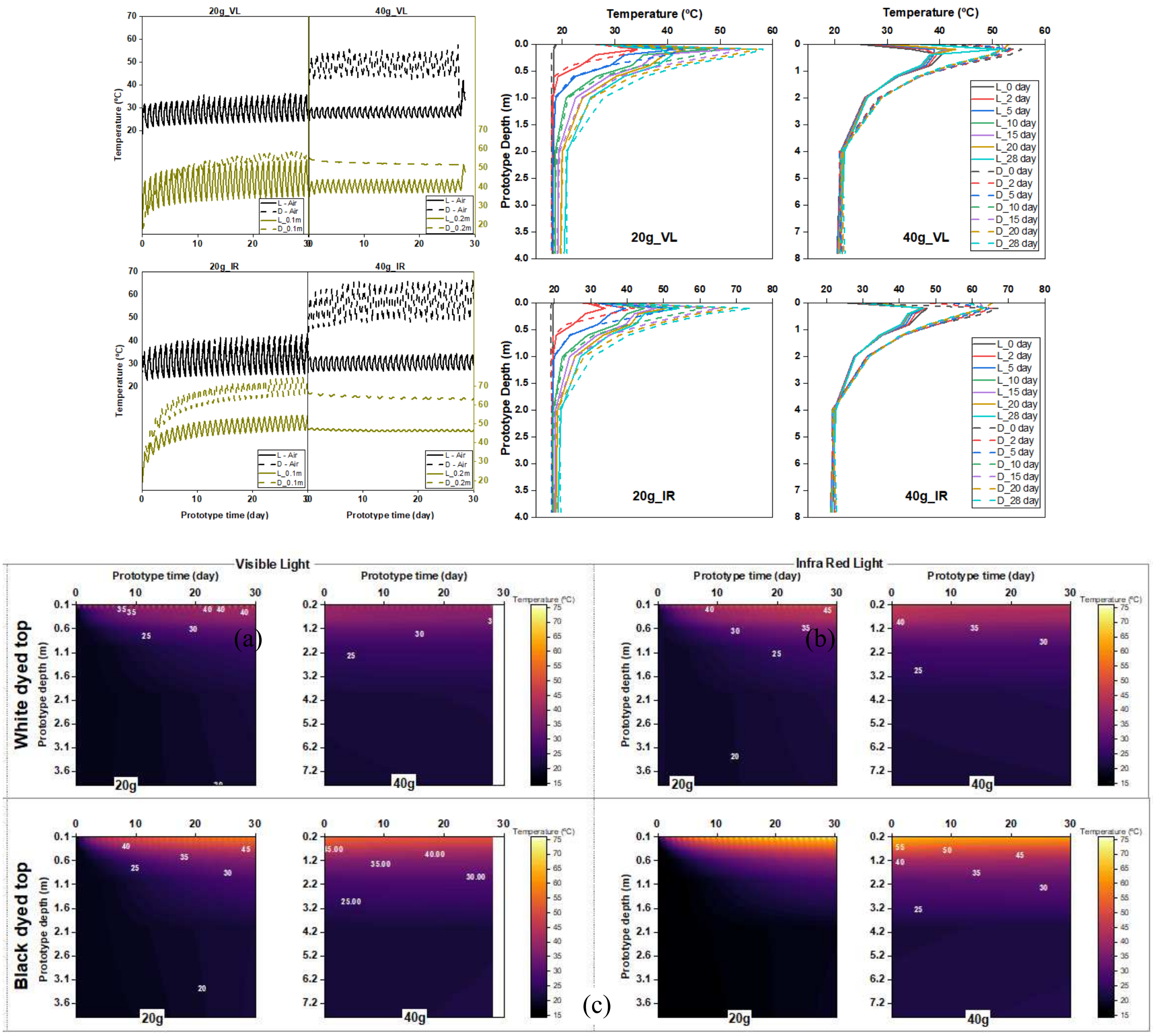

Figure 5. Thermal profiles at 20g and 40g with VL and IR heat lamps: (a) temperature vs time; (b) temperature vs depth; (c) heat contour map.

7 DISCUSSION

The experiments demonstrate that both surface albedo and forced convection induced by centrifuge spinning strongly influence thermal responses in soil columns, while depth plays a key role in modulating heat propagation. In all experimental configurations, the highest temperatures were consistently observed at the surface, followed by a sharp decline with depth. This trend indicates that radiative heating was largely confined to the near-surface region, with limited conductive heat transfer into the bulk material. The temperature fluctuations with depth reflects the soil's thermal inertia and matches classical observations of diurnal heat penetration in the near-surface soil layers (Popiel, Wojtkowiak and Biernacka, 2001; Ng *et al.*, 2015; Raouf *et al.*, 2015)

Under 1g conditions, surface and near-surface soil temperatures did not conform strictly to expectations based on albedo. While the dark-coloured column was expected to heat more due to greater radiative absorption, the light-coloured surface exhibited slightly higher temperatures. This was accompanied by larger cyclic variations in air temperature above the light surface (~20–63 °C) compared to the dark surface (~20–50 °C), indicating stronger surface–air thermal coupling over the light column. The rapid initial surface heating (18 → 50 °C in 10 min) followed by a slower rate beyond 20 min suggests that radiative absorption dominates early-stage heating, while convective and conductive losses gradually moderate temperature rise.

With increasing spin to 20g with VL lamp, forced convection became significant. Air temperature fluctuations above both columns decreased, reflecting enhanced air mixing within the centrifuge. Under these conditions, the dark column exhibited higher soil temperatures than the light column, conforming to expected albedo-driven heating. This difference was most pronounced within 0.5 m depth and decreased sharply beyond 2 m, indicating that subsurface thermal gradients are governed by radiative absorption and intrinsic soil properties, while airflow moderates the air temperature response.

At 40g with VL lamp, the impact of forced convection intensified. Air above the light column experienced a sudden cooling, while air above the dark column warmed sharply. The light surface experienced rapid cooling due to convective removal of heat, whereas the dark surface retained and redistributed absorbed energy, leading to elevated air temperatures above it. Surface soil temperatures responded similarly with sudden smaller dip and gradually declined during the test. Despite this, soil temperatures at depth remained largely consistent with 20g results, with pronounced differences only within the upper 0.5 m and uniform profiles beyond ~4 m.

The experiments under the IR lamp showed similar trends to VL illumination but with higher magnitudes, reflecting greater absorption of infrared radiation by soil.

The results underscore that, while albedo controls the potential for radiative heating, the presence of forced airflow and convective mixing can significantly alter near-surface temperature dynamics

8 FUTURE WORKS

The experiments were conducted with dry sand and an open-box configuration, which allowed forced convection and excluded moisture effects. Future work could investigate different saturation conditions, use a top plate to isolate radiation, and refine instrumentation to improve subsurface thermal measurements.

9 CONCLUSIONS

This study investigated the thermal response of light- and dark-coloured soil columns under visible and infrared irradiation across 1g, 20g, and 40g conditions. The results demonstrate that surface temperature evolution is governed by a combined influence of radiative input, surface albedo, forced convection, and depth-dependent thermal diffusion.

Under 1g conditions, thermal behaviour did not strictly follow albedo-based expectations, with comparable surface temperatures observed for both columns due to strong surface–air coupling in the absence of wind. Increasing Ng introduced significant forced convection, which reduced effective radiative heat input, moderated air temperature fluctuations, and altered surface thermal responses. Pyranometer measurements confirmed a substantial reduction in received heat energy with increasing Ng, highlighting the dominant role of centrifuge-induced airflow.

Across all conditions, temperature variations were confined primarily to the near-surface region, with the strongest gradients occurring within the upper 0.5 m and diminishing rapidly with depth. Beyond 2–4 m, soil temperatures remained largely unaffected by surface conditions. Infrared irradiation produced qualitatively similar trends to visible light but at higher temperature magnitudes.

Overall, the findings emphasize that while surface albedo controls radiative absorption potential, forced convection under high-g conditions can significantly modify the effective thermal boundary conditions. These results underscore the importance of accounting for airflow effects when interpreting thermal behaviour in centrifuge experiments and when extrapolating such data to natural or planetary surface environments.

ACKNOWLEDGEMENTS

The authors gratefully acknowledge the University of Sheffield for its support. Special thanks are extended to the technical team for their assistance and to former MSc student Haziq Al-Sadiqin Mohamed Bakri for his contribution to the initial stages of this research.

REFERENCES

Ali, N. et al. (2024). Comprehensive analysis of thermo-mechanical responses in collapsible soil under varied water content conditions. *Journal of Thermal Analysis and Calorimetry*, 149(23): 13721–13735. https://doi.org/10.1007/s10973-024-13439-3

Askarinejad, A. et al. (2012). Physical modelling of rainfall induced landslides under controlled climatic conditions. *2nd Eurofuge Conference on Physical Modelling in Geotechnics*, Deltares, Delft, Netherlands. http://www.cces.ethz.ch/projects/hazri/tramm/

Benson, D. O. and Dirmeyer, P. A. (2021). Characterizing the relationship between temperature and soil moisture extremes and their role in the exacerbation of heat waves over the contiguous United States. *Journal of Climate*, 34(6): 2175–2187. https://doi.org/10.1175/JCLI-D-20-0440.1

Blight, G. E. (2013). *Unsaturated Soil Mechanics in Geotechnical Practice*, 1st edn. London: CRC Press. https://doi.org/10.1201/b15239

Brandon, T. L. and Mitchell, J. K. (1989). Factors influencing thermal resistivity of sands. *Journal of Geotechnical Engineering*, 115(12): 1683–1698. https://doi.org/10.1061/(ASCE)0733-9410(1989)115:12(1683)

Campbell, G. S. and Norman, J. M. (1998). Heat flow in the soil. In: *An Introduction to Environmental Biophysics*, Springer, New York, NY. https://doi.org/10.1007/978-1-4612-1626-1_8

Casarella, A., Tarantino, A. and Di Donna, A. (2020). Micromechanical interpretation of thermo-plastic behaviour of clays. *E3S Web of Conferences*, Indonesia, pp. 09003. https://doi.org/10.1051/e3sconf/202020509003

Coccia, C. J. R. and McCartney, J. S. (2016). Thermal volume change of poorly draining soils I: Critical assessment of volume change mechanisms. *Computers and Geotechnics*, 80: 26–40. https://doi.org/10.1016/j.compgeo.2016.06.009

IPCC. (2023). *Climate Change 2021 – The Physical Science Basis: Working Group I Contribution to the Sixth Assessment Report of the Intergovernmental Panel on Climate Change*, 1st edn. Cambridge: Cambridge University Press. https://doi.org/10.1017/9781009157896

Laloui, L. (2001). Thermo-mechanical behaviour of soils. *Revue française de génie civil*, 5(6): 697–717. https://doi.org/10.3166/rfgc.5.697-717

Loria, R. A. F. and Coulibaly, J. B. (2021). Thermally induced deformation of soils: A critical overview of phenomena, challenges and opportunities. *Geomechanics for Energy and the Environment*, 25: 100193. https://doi.org/10.1016/j.gete.2020.100193

Madabhushi, G. (2017). *Centrifuge Modelling for Civil Engineers*, 1st edn. CRC Press. https://doi.org/10.1201/9781315272863

Mitchell, J. K. and Soga, K. (2005). *Fundamentals of Soil Behavior*. New York: John Wiley and Sons

Murashov, V. V. and White, M. A. (2000). Thermal conductivity of crystalline particulate materials. *Journal of Materials Science*, 35(3): 649–653. https://doi.org/10.1023/A:1004784613181

Ng, C. W. W. et al. (2015). Centrifuge modelling of heating effects on energy pile performance in saturated sand. *Canadian Geotechnical Journal*, 52(8): 1045–1057. https://doi.org/10.1139/cgj-2014-0301

Popiel, C. O., Wojtkowiak, J. and Biernacka, B. (2001). Measurements of temperature distribution in ground. *Experimental Thermal and Fluid Science*, 25(5): 301–309. https://doi.org/10.1016/S0894-1777(01)00078-4

Raouf, A. M. I. et al. (2015). Energy piles: Current state of knowledge and design challenges. *Environmental Geotechnics*, 2(4): 195–210. https://doi.org/10.1680/envgeo.13.00019

Smits, K. M. et al. (2010). Thermal conductivity of sands under varying moisture and porosity in drainage–wetting cycles. *Vadose Zone Journal*, 9(1): 172–180. https://doi.org/10.2136/vzj2009.0095

Warke, P. A. and Smith, B. J. (1998). Effects of direct and indirect heating on the validity of rock weathering simulation studies and durability tests. *Geomorphology*, 22: 347–357